Short communication

Effects of coal syngas major compositions on Ni/YSZ anode-supported solid oxide fuel cells

He Miao, Wei Guo Wang, Ting Shuai Li, Tao Chen, Shan Shan Sun, Cheng Xu*

Division of Fuel Cell and Energy Technology, Ningbo Institute of Materials Technology & Engineering, Chinese Academy of Sciences, Ningbo 315201, China

ARTICLE INFO

ABSTRACT

This paper presents a systematical evaluation of the effects of CO_2, H_2O, CO, N_2 and CH_4 in the coal syngas on the properties of typical Ni/YSZ anode-supported solid oxide fuel cells (SOFCs). The results show that CO_2, H_2O, CO, N_2 and CH_4 have complicated effects on the cell performance and the electrochemical impedance spectra (EIS) analysis reveals the addition of these gases influences electrode processes such as the oxygen ion exchange from YSZ to anode TPBs, the charge transfer at the anode TPBs, gas diffusion and conversion at the anode. Two kinds of mixture gases with different compositions are thus constituted and used as fuel for aging test on two cells at 750 °C. No degradation or carbon deposition is observed for the cell fueled with 40% H_2–20% CO–20% H_2O–20% CO_2 for 360 h while the cell fueled with 50% H_2–30% CO–10% H_2O–10% CO_2 exhibits an abrupt degradation after 50 h due to the severe carbon deposition.

© 2009 Elsevier B.V. All rights reserved.

1. Introduction

Solid oxide fuel cells (SOFCs) have attracted much attention because of their high efficiency, significant environmental benefits and good flexibility to fuel gases [1]. The SOFCs can reach electrical efficiencies of 45–60% and total efficiencies of 80% with cogeneration of heat and power [2]. Their high operation temperature makes the need of precious metal catalysts negligible, and they can run on a wide range of fuels, such as natural gas, biogas, methanol and coal syngas [3,4]. It is thus well believed that the SOFC technology is a bridge between fossil energy and hydrogen energy.

Coal syngas with H_2, CO, CO_2, H_2O, N_2 and CH_4 as major compositions is a fuel of rich resources and low cost, therefore, its use for SOFC as fuel has gained increasing interest [5–10]. However, there are two concerns on the application of coal syngas as fuel for SOFC. Firstly, some traces of impurities in the coal syngas such as H_2S, HCl, Cl_2 and PH_3 can poison the anode of SOFCs [11,7,12,13], resulting in performance degradation of the cell. Secondly, the CO tends to disproportionate due to the catalysis of Ni [14] when the SOFCs are fueled with some coal syngases at high temperatures, i.e. 600–900 °C, which leads to significant carbon deposition on the anode surface. In addition, this disproportionation reaction is exothermic [14], thus the carbon deposition becomes much more serious for the SOFCs operated at intermediate or low temperatures. Carbon deposition deactivates the anodes by increasing the

polarization resistance, reducing porosity and blocking active sites [15], which results in failure of the cell.

For coal syngas, carbon is formed from the disproportionation reaction (Eq. (1)) or CO reduction (Eq. (2)) [15]:

$$2CO = CO_2 + C \tag{1}$$

$$CO + H_2 = C + H_2O \tag{2}$$

The extent of each reaction depends on the temperature and gas composition. Different strategies have been developed to prevent carbon deposition on the anode surface of SOFC. Weber et al. [8] reported that a sufficient amount of water vapor and carbon dioxide in the loaded work anode could inhibit the formation and deposition of carbon, but a large amount of H_2O and CO_2 may reduce the real fuel proportion and cast a detrimental effect on the SOFCs. Nevertheless, it is possible to adjust coal syngas compositions to a certain extent so that the SOFCs operated using these "depleted-syngas" [10] can achieve high energy conversion efficiency and no carbon deposition at the same time. Burnette et al. [10] indicated that SOFC could operate using a "depleted-syngas" with the composition of 14.2% H_2–18.5% H_2O–43.1% CO–17.6% CO_2–6.6% N_2, however, no long-term cell performance was presented which is most important if slow carbon deposition exists.

The present investigation was thus initiated to give a comprehensive evaluation on the effect of each composition in the coal syngas, especially H_2O, CO_2, CO, N_2 and CH_4, on the properties of SOFCs. Based on these investigations, two kinds of syngas with compositions of 40% H_2–20% CO–20% H_2O–20% CO_2 and 50% H_2–30% CO–10% H_2O–10% CO_2 were designed and used as fuels for typical Ni/YSZ anode-supported single cells for durability evaluation.

2. Experimental

Experiments were carried out on flat plate anode-supported cells having dimensions of 5 cm × 5.8 cm with an active area of 4 cm × 4 cm. A Ni/8 mol% Y_2O_3-doped ZrO_2 (Ni/8YSZ) anode substrate of 400 μm thick was prepared by tape casting. An anode functional layer (Ni/YSZ) of 10 μm in thickness, an electrolyte layer (8YSZ) of 10 μm in thickness and a cathode including a LSM ($La_{0.75}Sr_{0.25}MnO_3$) active layer and a LSM current-collecting layer were sprayed on the anode substrate one by one followed by co-sintering.

The cells were tested by mounting in an identical alumina testing house and using silicon dioxide as sealant. Platinum foil was employed as current collector at cathode side while nickel foil was used as current collector at anode side. Silver mesh sandwiched LSM and two layer nickel foams were utilized for gas distribution at cathode side and anode side, respectively. The cells were then placed into a furnace and heated to 850 °C in N_2 with a heating rate of 1 °C min^{-1}. The reduction of the NiO–YSZ was performed under pure hydrogen with a flow rate of 0.3 SLM (standard liter per minute) for more than 5 h. After reduction, the furnace temperature was decreased to 750 °C for testing. The air with a flow rate of 2 SLM and pure H_2 with a flow rate of 0.5 SLM were used as cathode oxidant and anode fuel gas, respectively. The cell was discharged galvanostatically at 0.5 A cm^{-2} for 24 h to ensure full electrode activation [16].

I–V curves and electrochemical impedance spectrum (EIS) were obtained when the single cell was fueled with 0.3 SLM H_2. The vapor, CO_2, N_2 and CH_4 were added in the fuel gas with the flow rate for H_2 unchanged, respectively. Each gas mentioned above had a volume fraction of 10%. The mixture gases having a composition of 70% (CO + H_2)–25% CO_2–5% H_2O was injected into the anode of SOFC with a flow rate of 0.5 SLM where the CO content varied from 0% to 70% in order to study the role of CO on the properties of SOFCs. All EIS curves were obtained at open circuit voltage (OCV) by four-electrode configuration using an Electrochemical Workstation (IM6ex, ZAHNER) with a scanning frequency range from 0.01 Hz to 1 MHz.

Aging tests were performed with a current density of 0.5 A cm^{-2} at 750 °C on two SOFC single cells (denoted as cell 1 and cell 2) using two kinds of simulated coal syngases (40% H_2–20% CO–20% H_2O–20% CO_2 and 50% H_2–30% CO–10% H_2O–10% CO_2) as fuel. Both the two kinds of simulated coal syngases had a flow rate of 0.5 SLM. Anodic microstructures of the cells after aging test were observed by a HITACHI S4800 Scanning Electron Microscope (SEM).

3. Results

3.1. Electrochemical properties

Fig. 1 shows I–V curves of an anode-supported SOFC single cell fueled with H_2/H_2O/CO_2 mixture gases at 750 °C. It can be seen that the OCV of the single cell decreases with the addition of 10% H_2O and CO_2 into the pure H_2. The OCV of the cell fueled with 90% H_2–10% CO_2 is 990 mV, which is much lower than that of the cell fueled with pure H_2 (1074 mV). The P_{max} of the single cell increases from 316 to 325 mW cm^{-2} with the addition of 10% H_2O to pure H_2, while the P_{max} decreases with the addition of 10% CO_2 because of the much lower OCV. In addition, the slope of the I–V curves at high current densities (>0.6 A cm^{-2}) becomes smaller with the addition of the above gases, especially H_2O, which indicates the proper addition of H_2O and CO_2 can decrease the concentration polarization effectively. Fig. 2 shows the EIS curves of the SOFC single cell fueled with different ratios of H_2/H_2O/CO_2 at 750 °C. It can be seen that the polarization resistance (R_p) decreases with the
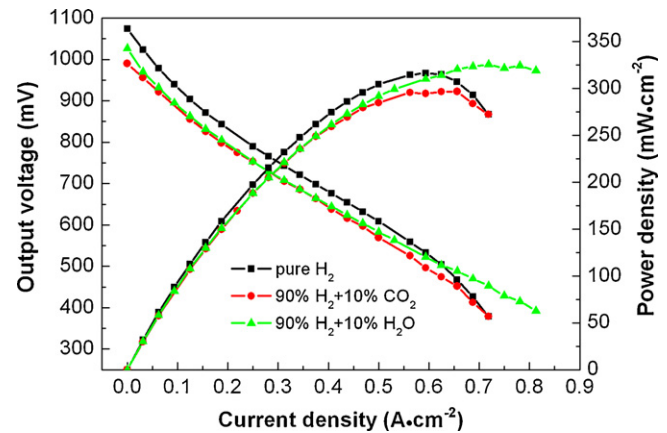
Fig. 1. I–V curves of a 4 cm × 4 cm anode-supported SOFC single cell fueled with H_2/H_2O/CO_2 mixture gases at 750 °C.
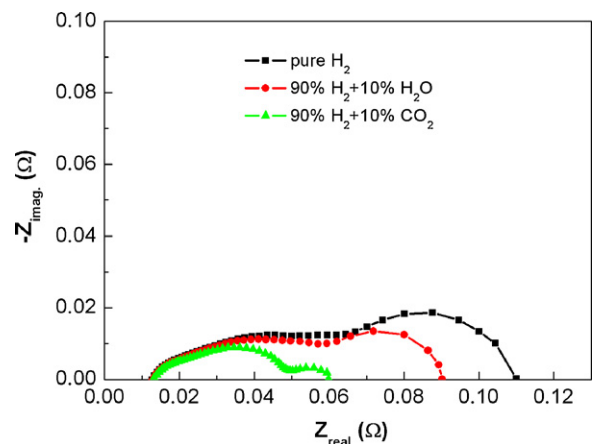
Fig. 2. EIS (Nyquist plots) of a 4 cm × 4 cm anode-supported SOFC single cell fueled with H_2/H_2O/CO_2 mixture gases at 750 °C.

addition of H_2O/CO_2. The R_p obtained at 90% H_2–10% CO_2 mixture gas is 60 mΩ which is much smaller than that operated with pure H_2 (110 mΩ).

Fig. 3 shows the I–V properties of the single cell fueled with x% H_2–$(70 - x)$% CO–5% H_2O–25% CO_2 (x = 0–70) mixture gases at 750 °C. Here, on the purpose of suppressing the severe carbon deposition caused by the disproportionation reaction of CO, a proper portion of CO_2 and H_2O were added into the H_2–CO mixture gases.
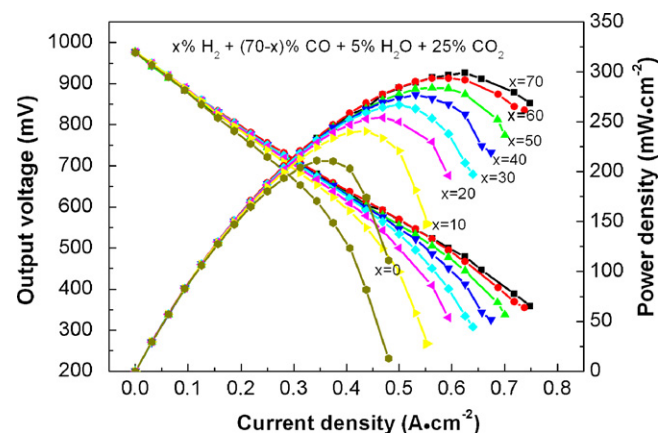
Fig. 3. I–V curves of a 4 cm × 4 cm anode-supported SOFC single cell fueled with x% H_2–$(70 - x)$% CO–5% H_2O–25% CO_2 (x = 0–70) mixture gases at 750 °C.
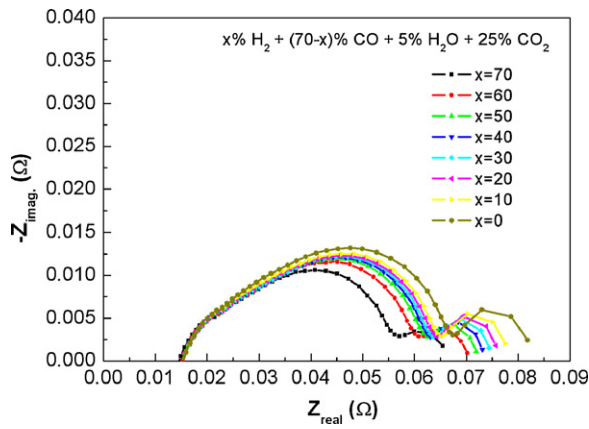
Fig. 4. EIS (Nyquist plots) of a 4 cm × 4 cm anode-supported SOFC single cell fueled with $x\%$ H_2–$(70 - x)\%$ CO–5% H_2O–25% CO_2 ($x = 0$–70) mixture gases at 750 °C.

It can be seen that the OCV values of the single cell fueled with different ratios of H_2 to CO are almost the same, about 976 mV. The P_{max} decreases from 299 to 211 mW cm^{-2} with increasing CO content from 0% to 70%. Also, the slope of I–V curves at high current densities increases with the increase of CO content, which indicates that the concentration polarization increases. In addition, as can be seen from Fig. 4, the R_p increases from 65.5 to 81.8 mΩ with increasing CO content from 0% to 70%.

Fig. 5 shows the I–V properties of the single cell fueled with H_2/N_2/CH_4 mixture gases at 750 °C. The OCV of the single cell decreases with the addition of 10% N_2 to the pure H_2 but increases to 1218 mV with the injection of 10% CH_4. However, the P_{max} of the single cell decreases with the injection of either N_2 or CH_4 into the pure H_2. The P_{max} is 197 mW cm^{-2} for the single cell fueled with 90% H_2–10% CH_4, which is about 80 mW cm^{-2} lower than that of the cell fueled with pure H_2. From EIS curves as shown in Fig. 6 for the cell fueled with H_2/N_2/CH_4 mixture gases, it can be seen that the addition of N_2 or CH_4 into pure H_2 increases the R_p of the single cell. The R_p of the single cell fueled with 90% H_2–10% CH_4 reaches 294 mΩ.

3.2. Degradation behaviors

The results from Section 3.1 indicated that CO, N_2 and CH_4 had the negative effects on the single cell. Considering the small amount of N_2 and CH_4 (the volume fractions of them are usually less than 5%) in the coal syngas, the mixture gases being developed in this
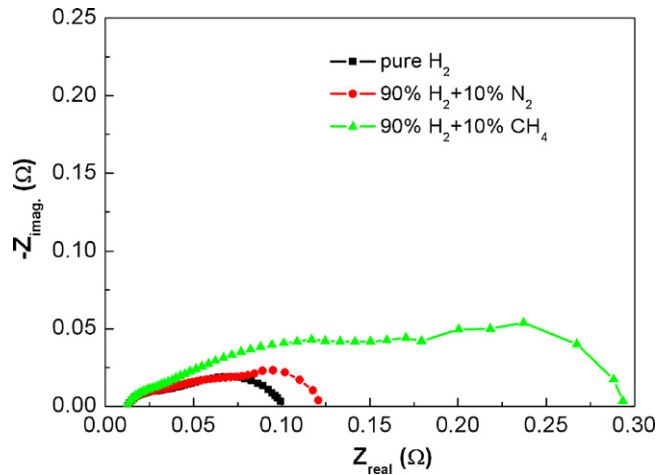

Fig. 6. EIS (Nyquist plots) of a 4 cm × 4 cm anode-supported SOFC single cell fueled with H_2/N_2/CH_4 mixture gases at 750 °C.

section were designed with the elimination of N_2 and CH_4. Two kinds of "depleted syngas" with the compositions of 40% H_2–20% CO–20% CO_2–20% H_2O and 50% H_2–30% CO–10% CO_2–10% H_2O were thus developed.

Fig. 7 shows the ageing testing results for two cells (denoted as cell 1 and cell 2) fueled with different ratios of H_2–CO–CO_2–H_2O simulated coal syngases with a current load of 0.5 A cm^{-2} at 750 °C. It has to be noted that the two full cells showed different performances prior to aging test: the cell 1 has a P_{max} value of 550 mW cm^{-2} at 750 °C when fueled with 0.8 SLM pure H_2 while the cell 2 exhibits a P_{max} of 300 mW cm^{-2}. During the aging test, as can be seen from Fig. 7, the output voltage of cell 1 fueled with 40% H_2–20% CO–20% CO_2–20% H_2O increases gradually from 683 to 735 mV after 360 h, and no degradation can be found. Whereas, the output voltage of cell 2 fueled with 50% H_2–30% CO–10% CO_2–10% H_2O decreases at a constant rate for about 50 h after activation and then abruptly drops to 189 mV. Koch et al. [17] reported that a voltage limit for the SOFCs existed and the degradation became significant when the output voltage was below this value. The voltage limit which might be related to the anode polarization was about 750 mV at 750 °C. For cell 2, the output voltage is much lower than 750 mV, which might be an explanation for its quick degradation.
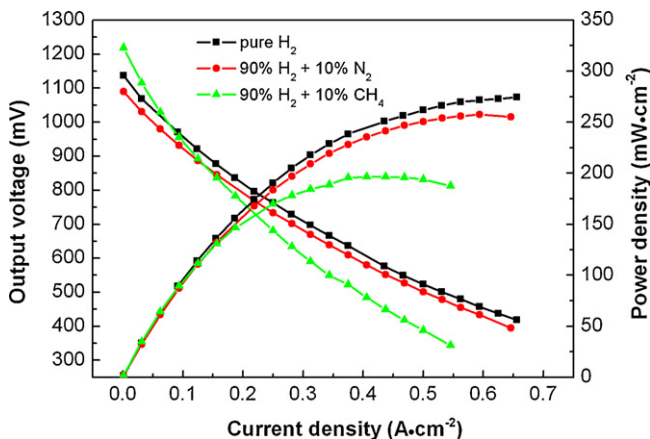

Fig. 5. I–V curves of a 4 cm × 4 cm anode-supported SOFC single cell fueled with H_2/N_2/CH_4 mixture gases at 750 °C.
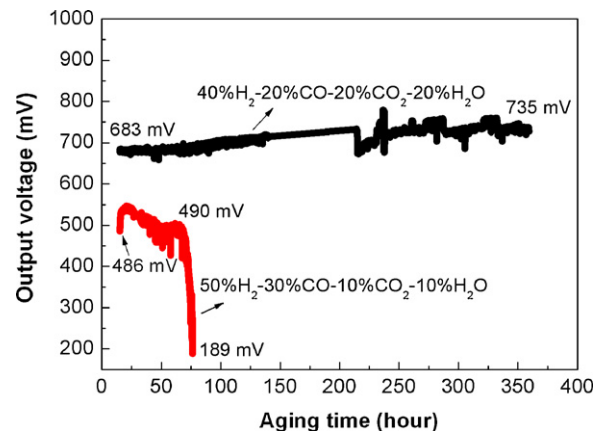

Fig. 7. Cell output voltage versus operation time for 4 cm × 4 cm anode-supported SOFC single cells fueled with different ratios of H_2–CO–CO_2–H_2O mixture gases under a constant current load of 0.5 A cm^{-2} at 750 °C.

Table 1
Summary of the effects of CO_2, H_2O, CO, N_2 and CH_4 on the major electrochemical properties of SOFC single cell.

Composition	OCV (mV)	ASR (Ω cm^2)	P_{max} (mW cm^{-2})	R_p (Ω)	Zone (Hz)
CO_2	–	○	–	–	<1000
H_2O	–	○	+	–	<1000
CO	○	+	–	+	<10,000
N_2	–	○	+	+	<10
CH_4	+	+	–	+	<3000

Note: Zone denotes frequency deviation zone of Z_{real} in Fig. 8, "–" denotes decrease, "○" denotes slight change or no change and "+" denotes increase.

4. Discussion

4.1. Effects on open circuit voltage and electrode processes

Table 1 summaries the effects of CO_2, H_2O, CO, N_2 and CH_4 on the major electrochemical properties of SOFC single cells where area specific resistance (ASR) is calculated by $(OCV - 0.7)/I_{0.7}$. $I_{0.7}$ denotes the current density corresponding to an output voltage of 0.7 V. Apparently, the CO_2, H_2O and N_2 contents in coal syngas have a negative effect on the OCV of the single cell whereas the CO content has no effect on the OCV and the CH_4 content increases the OCV. The OCV value is very close to the electromotive force (e.m.f.) which can be calculated by Eq. (3) [18]

$$\text{e.m.f.} = \frac{RT}{4F} \ln \frac{p'_{O_2}}{p''_{O_2}} \tag{3}$$

where F, R, T, p'_{O_2} and p''_{O_2} are the Faradic constant, gas constant, absolute temperature, the partial pressure of oxygen on the cathode and the partial pressure of oxygen on the anode, respectively. Generally speaking, p'_{O_2} is equivalent to 1 atm so that the e.m.f. is determined by p''_{O_2}. When the anode fuel gas of SOFC is H_2, the anode reaction can be described as Eq. (4), and then p''_{O_2} can be calculated by Eq. (5) [18].

$$H_2 + O^{2-} = H_2O + 2e^- \tag{4}$$

$$p''_{O_2} = \left[\frac{p_{H_2O}}{p_{H_2}} \exp\left(\frac{\Delta G^a}{RT} \right) \right]^2 \tag{5}$$

where ΔG^a, p_{H_2O}, p_{H_2} is free energy change of Eq. (4), partial pressure of H_2O and partial pressure of H_2, respectively. The ΔG^a is calculated to be −196.4 kJ here using the Gibbs–Helmholtz equation. When CO_2, H_2O and N_2 are injected into the pure H_2, they cannot react with O^{2-} on the anode three phase boundaries (TPBs). According to Eq. (5), the p_{H_2} will decrease, which can cause an increase of p''_{O_2}. From Eq. (3), e.m.f. decreases with the increase of p''_{O_2}, which may be an explanation of the decrease of OCV with the addition of CO_2, H_2O and N_2.

When CO is used as anode fuel gas, the anode reaction can be described as Eq. (6), and Eq. (5) becomes Eq. (7) by substituting p_{H_2O} and p_{H_2} with p_{CO_2} and p_{CO}, respectively.

$$CO + O^{2-} = CO_2 + 2e^- \tag{6}$$

$$p''_{O_2} = \left[\frac{p_{CO_2}}{p_{CO}} \exp\left(\frac{\Delta G^b}{RT} \right) \right]^2 \tag{7}$$

In Eq. (7), ΔG^b is free energy change of Eq. (6) and calculated to be −194.2 kJ. The values of $\exp(\Delta G^a/RT)$ and $\exp(\Delta G^b/RT)$ in Eqs. (5) and (7) are 0.9772 and 0.9774, respectively. Assuming temperature and external pressure is the same for oxidation reactions of H_2 and CO, Eq. (7) is in a similar form to Eq. (5). The calculated e.m.f. value and thus the OCV remain constant as long as the total amount of fuel is constant, which is the experimental setting for
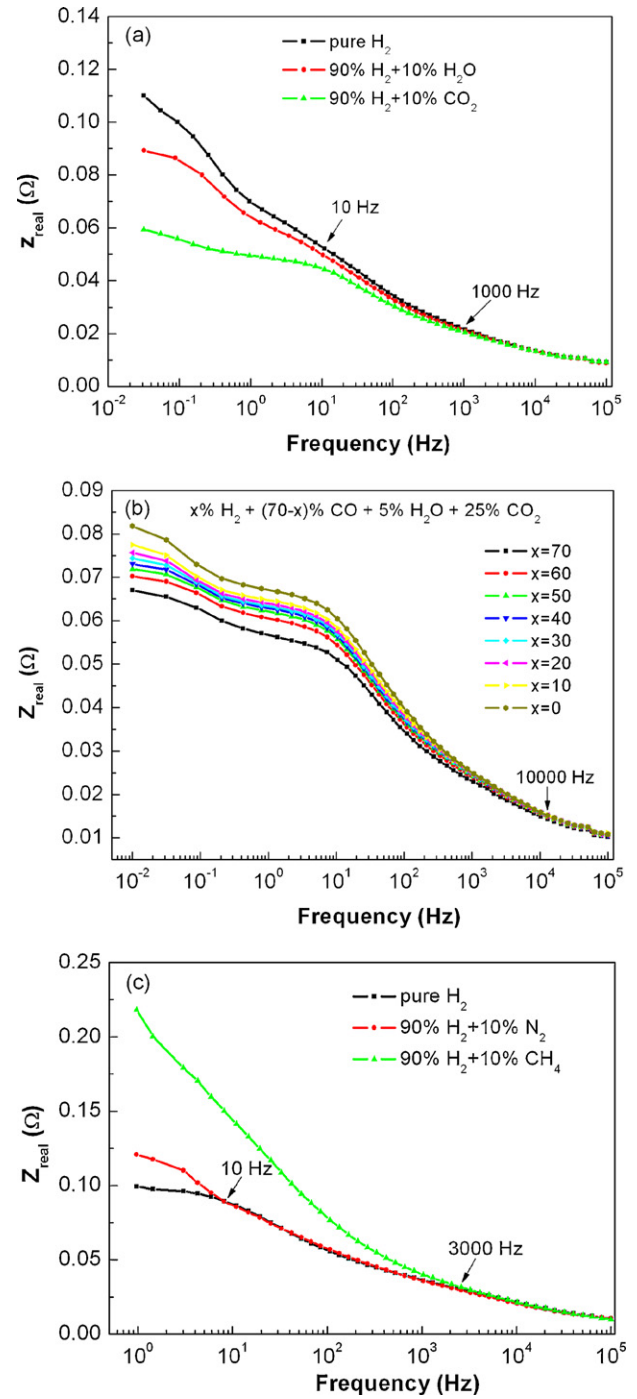
Fig. 8. Variation of Z_{real} with frequency of a 4 cm × 4 cm anode-supported SOFC single cell fueled with different fuel gases: $H_2/CO_2/H_2O$ (a); x% H_2–(70 − x)% CO–5% H_2O–25% CO_2 (x = 0–70) (b); $H_2/N_2/CH_4$ (c).

the present investigation. Therefore, the OCV exhibits no change with the addition of CO into the fuel gases.

When CH_4 is used as anode fuel gas, the anode reaction is more complicated than that of H_2 and CO. As the ratio of O_2 to CH_4 (x) is low, methane cracking reaction (Eq. (8)) takes place; as x increases up to 0.5, electrochemical partial oxidation reaction (Eq. (9)) takes place; as x increases above 0.5, the reaction becomes complete oxidation, i.e. Eq. (10) [19].

$$CH_4 = C + 2H_2 \tag{8}$$

$$CH_4 + O^{2-} = 2H_2 + CO + 2e^- \tag{9}$$
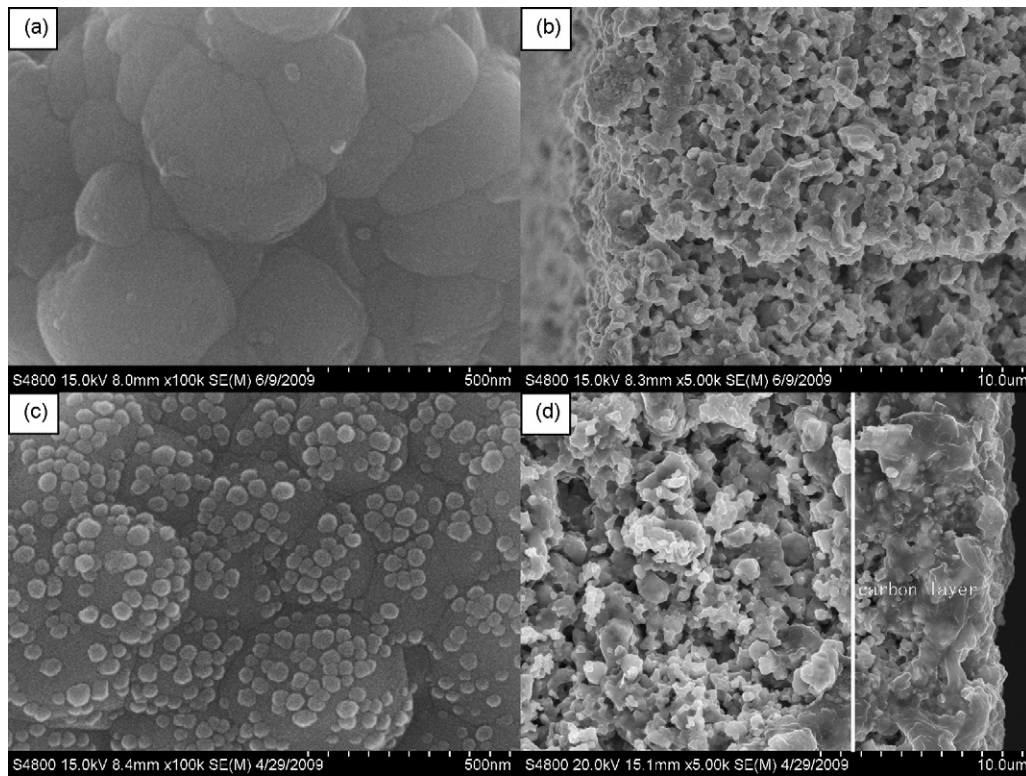
Fig. 9. SEM micrographs of the SOFC single cells using different ratios of H_2–CO–CO_2–H_2O mixture gases as fuel under constant current load of 0.5 A cm^{-2} at 750 °C: surface (a) and cross-section (b) of cell 1 fueled with 40% H_2–20% CO–20% CO_2–20% H_2O for 360 h; surface (c) and cross-section (d) of cell 2 fueled with 50% H_2–30% CO–10% CO_2–10% H_2O for 76 h.

$$\frac{1}{4}CH_4 + O^{2-} = \frac{1}{2}H_2O + \frac{1}{4}CO_2 + 2e^- \tag{10}$$
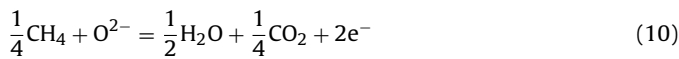
Assuming x is more than 0.5 as the general condition in the present investigation, the p''_{O_2} can be calculated by Eq. (11):

$$p''_{O_2} = \left[\frac{p_{CO_2}^{1/4} p_{H_2O}^{1/2}}{p_{CH_4}^{1/4}} \exp\left(\frac{\Delta G^c}{RT}\right) \right]^2 \tag{11}$$

where ΔG^c is the free energy change of complete oxidation reaction of CH_4 which is −199.2 kJ. Apparently, Eqs. (5) and (7) are different from Eq. (11) in exponents, therefore, the change in p''_{O_2} due to the introduction of CH_4 into the fuel is very different from the change in p''_{O_2} corresponding to the decrease in fuel amount besides CH_4, that is H_2 and/or CO. It is thus difficult to estimate the change of OCV from Eq. (11) with the addition of CH_4 into the fuel gases. Lin et al. [19] reported that the OCV of SOFC fueled with pure CH_4 was much higher than that fueled with pure H_2 at 750 °C, which is in accord with our results.

It is well believed that the resistance of a SOFC single cell (R_{cell}) is the sum of a number of contributions, which can be determined by EIS. The resistance of the cell can thus be described using Eq. (12) [20]:

$$R_{cell} = R_{elec} + R_{cath} + R_{ano} + R_{conc} \tag{12}$$

where R_{elec} is the resistance of the electrolyte, R_{cath} and R_{ano} are the chemical and electrochemical losses at the cathode and anode, respectively, and R_{conc} denotes the diffusion and gas conversion losses at the anode. The latter three components, R_{cath}, R_{ano}, and R_{conc}, cover the polarization losses.

These losses can be further broken down into electrode processes by EIS curves analysis according to frequency zone of each arc, i.e. transport of O-intermediates at LSM–YSZ interface, charge transfer between Ni and YSZ, dissociative adsorption of O_2 and

transport to TPB, diffusion and gas conversion at anode [20–22]. Previous experimental results indicated that the frequencies at the arc summits (f_{summit}) corresponding to the above electrode processes are 12,000–62,000, 1500–10,000, 150–1100 and below 50, respectively, when the temperature ranged from 700 to 850 °C.

Fig. 8 shows the relations of frequency and Z_{real} of the cell fueled with H_2/H_2O/CO_2/CO/N_2/CH_4 mixture gases. The frequency deviation zones of Z_{real} from Fig. 8 are also listed in Table 1. As can be seen from Fig. 8(a) and Table 1, the difference between Z_{real} for H_2/CO_2/H_2O mixture gases with pure H_2 become significant at frequencies below 10 Hz, which corresponds to the gas diffusion and conversion [23–25]. In addition, the Z_{real} obtained at H_2/H_2O/CO_2 mixture gases are slightly different at the frequency zone of 1000–10 Hz. This frequency zone can be ascribed to the dissociative adsorption of O_2 followed by the electrochemical reduction and transfer of oxygen species at the TPBs [23]. It is not clear the effect of water on the electrode processes, however, Hendriksen et al. [26] reported that H_2O can decrease the anode gas diffusion losses. Sakai et al. [27,28] also reported the fast interaction between H_2O molecule and oxygen ion in electrolytes (Eq. (13)) was dominant in a humid atmosphere resulting in apparent high surface exchange rate of oxygen ion.

$$H_2O_{ad} + O^{2-} \text{ (in YSZ)} = 2OH^- \text{ (on YSZ)} \tag{13}$$

Since this equation is reversible, the fuel gas can react with the oxygen ion from OH$^-$ at the TPB preferentially. The diffusion and transfer of oxygen ion from the YSZ to anode TPBs may thus become less dominant, which may be an explanation for the decrease of concentration polarization with the addition of H_2O. Similarly, CO_2 may have similar effect as H_2O on the properties of the SOFCs.

As shown in Fig. 8(b) and (c), Z_{real} for the cell fueled with x% H_2–(70 − x)% CO–5% H_2O–25% CO_2 (x = 0–70) and 90% H_2–10% CH_4 mixture gases becomes different from Z_{real} for the cell fueled

with pure H_2 when the frequency is less than 10,000 and 3000 Hz, respectively, which indicates that both charge transfer at the anode TPBs and the gas diffusion and conversion at anode become slower with the injection of CO and CH_4 in the fuel gas [20]. In addition, from Fig. 8(c), the deviation of Z_{real} occurs when the frequency is less than 10 Hz with the injection 10% N_2 into pure H_2. It is thus concluded that the addition of N_2 into the pure H_2 only affects the gas diffusion and conversion at anode [23].

4.2. Degradation mechanisms

As shown in Fig. 7, the two cells fueled with two different ratios of H_2–CO–CO_2–H_2O mixture gases exhibit different degradation behaviors. The anodic microstructures for these two as-tested cells are thus inspected at the surface and cross-section plane in Fig. 9. A rich carbon layer about 5 μm thick is observed at the anode surface of cell 2 fueled with 50% H_2–30% CO–10% CO_2–10% H_2O. This layer must be disadvantageous to the fuel gas diffusion from anode surface to TPBs. In addition, some "nano-particles" having sizes of about 50 nm are distributed on the surface of nickel in the anode. The "nano-particles" should be the deposited carbon or nickel carbide, which may greatly decrease the conductivity or activity of nickel in the anode. The formation of the carbon layer and "nano-particles" should be ascribed to the disproportionation reaction or CO reduction (Eqs. (1) and (2)) of CO [15]. For cell 1, no such carbon layer or "nano-particles" can be found on the anode surface. It is well known that H_2O and CO_2 can effectively suppress the carbon deposition at high temperatures by Eqs. (14)–(16) [29].

$$C + CO_2 = 2CO \tag{14}$$

$$C + H_2O = CO + H_2 \tag{15}$$

$$CO + H_2O = CO_2 + H_2 \tag{16}$$

Thus, no carbon layer or "nano-particles" on the anode surface of cell 1 can be related to the higher CO_2 and H_2O contents in the fuel gas.

From the degradation behavior of SOFCs operated under simulated coal syngas, we can find that the carbon deposition on the anode surface is fatal for the cell life. The deposited carbon increases the ohm resistance and polarization resistance by decreasing the conductivity or activity of nickel and blocking the pore of anode support. The carbon deposition may be caused by the disproportionation reaction or CO reduction and can be eliminated by increasing CO_2 and H_2O contents in the mixture gases, especially when the content of H_2O and CO_2 is somewhat larger than that of CO. So a proper increase of H_2O and CO_2 content in syngas can effectively improve the electrochemical properties of the single cell and suppresses the carbon deposition on the anode surface caused by CO.

5. Summary and conclusions

The effects of the H_2O, CO_2, CO, N_2 and CH_4 in the coal syngas on the SOFCs properties were systemically investigated and their mechanisms were discussed through individual electrode process analysis. It was found that the OCV of the cell decreased with the injection of N_2, CO_2 and H_2O while CO had no effect on the OCV. The OCV also increased with the injection of CH_4.

Proper H_2O and CO_2 contents in the coal syngas could decrease the concentration polarization and accelerate the oxygen ion exchange rate from YSZ to anode TPBs, and thus lead to a good cell performance. The CO and CH_4 slowed down the charge transfer at the anode TPB and the gas diffusion and conversion at anode, while N_2 affected the gas diffusion and conversion at anode.

A simulated coal syngas with compositions of 40% H_2–20% CO–20% H_2O–20% CO_2 was used as fuel for a typical anode-supported cell and no degradation or carbon deposition could be found in the cell operating at 750 °C for 360 h. Whereas, the single cell operated under 50% H_2–30% CO–10% H_2O–10% CO_2 showed an abrupt degradation due to the severe carbon deposition.

References

[1] S. Tao, J.T.S. Irvine, Nat. Mater. 2 (2003) 320.
[2] H. Yokokawa, H. Tu, B. Iwanschitz, A. Mai, J. Power Sources 182 (2008) 400.
[3] M.E. Perry, T. Tsai, S.A. Barnett, Nature 400 (1999) 649.
[4] S. Park, J.M. Vohs, R.J. Gorte, Nature 404 (2000) 265.
[5] R.S. Gemmen, J. Trembly, J. Power Sources 161 (2006) 1084.
[6] T.J. Huang, C.L. Chou, W.J. Chen, M.C. Huang, Electrochem. Commun. 11 (2009) 294.
[7] J.P. Trembly, R.S. Gemmen, D.J. Bayless, J. Power Sources 163 (2007) 986.
[8] A. Weber, B. Sauer, A.C. Muller, D. Herbstritt, E. Ivers-Tiffee, Solid State Ionics 152–153 (2002) 543.
[9] T. Kivisaari, P. Bjornbom, C. Sylwan, B. Jacquinot, D. Jansen, A. de Groot, Chem. Eng. J. 100 (2004) 167.
[10] D.D. Burnette, G.G. Kremer, D.J. Bayless, J. Power Sources 182 (2008) 329.
[11] C. Xu, J.W. Zondlo, H.O. Finklea, O. Demircan, M. Gong, X.B. Liu, J. Power Sources 193 (2009) 739.
[12] F.N. Cayan, M. Zhi, S.R. Pakalapati, I. Celik, N. Wu, R. Gemmen, J. Power Sources 185 (2008) 595.
[13] T.S. Li, H. Miao, T. Chen, W.G. Wang, C. Xu, J. Electrochem. Soc. 156 (2009) B1383.
[14] H. Nakano, S. Kawakami, T. Fujitani, J. Nakamura, Surf. Sci. 454–456 (2000) 295.
[15] V. Alzate-Restrepo, J.M. Hill, J. Power Sources (2009), doi:10.1016/j.jpowsour.2009.09.014.
[16] V.A.C. Haanappel, A. Mai, J. Mertens, Solid State Ionics 177 (2006) 2033.
[17] S. Koch, P.V. Hendriksen, M. Mogensen, N. Dekker, B. Rietveld, B. de Haart, F. Tietz, Proceedings of the 6th European Solid Oxide Fuel Cell Forum European Solid Oxide Fuel Cell Forum, Lucerne, Switzerland, 2004, p. 299.
[18] S.W. Zha, C.R. Xia, G.Y. Meng, J. Appl. Electrochem. 31 (2001) 93.
[19] Y. Lin, Z. Zhan, J. Liu, S.A. Barnett, Solid State Ionics 176 (2005) 1827.
[20] R. Barfod, A. Hagen, S. Ramousse, P.V. Hendriksen, M. Mogensen, Fuel Cells 6 (2006) 141.
[21] E.P. Murray, T. Tsai, S.A. Barnett, Solid State Ionics 110 (1998) 235.
[22] Q.A. Huang, R. Hui, B. Wang, J. Zhang, Electrochim. Acta 52 (2007) 8144.
[23] R. Barfod, M. Mogensen, T. Klemenso, A. Hagen, Y.L. Liu, P.V. Hendriksen, J. Electrochem. Soc. 154 (2007) B371.
[24] S. Primdahl, M. Mogensen, J. Electrochem. Soc. 146 (1999) 2827.
[25] S.B. Adler, J.A. Lane, B.C.H. Steele, J. Electrochem. Soc. 143 (1996) 3554.
[26] P.V. Hendriksen, S. Koch, M. Mogensen, Y.L. Liu, P.H. Larsen, Proceedings of the international symposium on solid oxide fuel cells VIII, The Electrochemical Society Proceedings Series, Pennington, USA, 2003, p. 1147.
[27] N. Sakai, K. Yamaji, H. Negishi, T. Horita, H. Yokokawa, Y.P. Xiong, M.B. Phillipps, Electrochemistry 68 (2000) 499.
[28] N. Sakai, K. Yamaji, T. Horita, Y.P. Xiong, H. Kishimoto, H. Yokokawa, J. Electrochem. Soc. 150 (2003) A689.
[29] W. Karchera, P. Glaudea, Carbon 9 (1971) 617.